Quantitative assessment of electrical, optical and recombination losses in heterojunction CdS/CdTe solar cells

H. A. MOHAMED[a], A. S. MOHAMED[b,c]
[a]*Physics department, Faculty of Science, Sohag University, 82524 Sohag, Egypt*
[b]*Department of Physics and Astronomy, College of Science, King Saud University, 11451 Riyadh, KSA*
[c]*Physics department, Faculty of Science, Al-Azhar University, Cairo, Nasr City, Egypt*

In this paper, electrical, optical and recombination losses in thin-film solar cells passed on CdS/CdTe have been evaluated. Electrical losses due to series and shunt resistances are quantitatively estimated from *J-V* curves. *J-V* characteristics are described in terms of the Sah– Noyce–Shockley theory of generation–recombination in the space-charge region of the CdS/CdTe heterostructure. Optical losses due to multiple reflections from the cell interfaces as well as absorption in the ITO and CdS layers are found using the refractive index and the extinction coefficient of the used materials. Losses arise from the recombination of the generated carriers at the front and rare surface of CdTe layer are carried out on the basis of the width of the space-charge region and other parameters of the absorber layer. It is found that the fill factor, output power density and the cell efficiency decreases with increasing the series resistance and decreasing the shunt resistance. The electrical losses due to series and shunt resistance are about 6%. Decreasing the thickness of window layer from 100 nm to 50 nm leads to increase the short-circuit current density from 23.6 mA/cm^2 to 24.8 mA/cm^2 and then reducing the optical losses from 24% to 20%. The recombination losses record a minimum value of 5% at width 1 μm of the space-charge region and record a maximum value of 27% at width=7μm.

(Received December 15, 2015; accepted April 6, 2017)

Keywords: CdS/CdTe solar cell, Optical losses, Recombination losses, Electrical losses, Cell efficiency

1. Introduction

The Cadmium telluride/Cadmium sulphide (CdS/CdTe) solar cells are one of the most promising thin–film solar cells. CdTe became a candidate for solar cells in the early 1950s due to its direct band gap of 1.5 eV which is very close to the optimum band-gap for solar cells [1]. CdTe has a high absorption coefficient over 5×10^5 cm^{-1} meaning that all the incident photons with energy greater than the band-gap can be absorbed within the first few microns of thickness of CdTe absorber layer [2].CdS has high optical band gap of 2.4 eV, thus the function of CdS is to allow energetic short-wavelength photons to pass for the incidence at the hetero-interface with minimum absorption loss. The other use of CdS is to provide a junction field for separation of photogenerated minority carriers before recombination [3].

The recorded CdS/CdTe cell efficiency remained 16.5% [4] for a decade, which was recently reported to be improved to 18.3% [5]. The theoretical efficiency of CdS/CdTe solar cells is predicted to be up to 28–30% [6,7].The major impact factors for this difference are due to the optical losses, recombination losses and electrical losses. It is reported that the optical losses are coming from the reflection between any two interfaces losses in the cell (air-glass, glass-TCO, TCO-CdS, CdS-CdTe) as well as the absorption losses in glass, TCO and CdS layers [8, 9]. The recombination losses are coming from the front surface recombination and back surface recombination of the absorber layer as well as the recombination in space-charge region [10]. Finally, the electrical losses are attributed to the series and shunt resistances in CdS-CdTe cell [11, 12]. To our knowledge, the effect of optical, electrical and recombination losses of CdS-CdTe solar cell were not studied theoretically in literatures.

In this paper, the effect of optical, recombination and electrical losses on the short-circuit current and on the cell parameters such as fill factor, open-circuit voltage, output power density and efficiency have been studied. The calculations carried out are based on the multiple reflections at the interface between any two layers, absorption losses in front-contact and window layers, front recombination at the CdTe/CdS interface, back recombination of absorber layer and electrical losses due to series and shunt resistances. The current study ignored the effect of recombination losses in space-charge region and the reflectivity from metallic back contact.

2. Theory

2.1. Electrical losses

The determination of the fill fact, open-circuit voltage, output power density and solar cell efficiency implies

knowledge of its *I–V* characteristic curve, the general form of which can be written as:

$$J(V) = J_d - J_{ph} \tag{1}$$

where J_d is the dark current density and J_{ph} is the photocurrent density. In the current calculation we assumed that the photocurrent density J_{ph} equals the short-circuit current density J_{SC}. It was reported [13-15] that the Sah–Noyce–Shockley generation–recombination theory is considered the actual method to describe the dark current in CdS-CdTe solar cells. According to the Sah–Noyce–Shockley theory, the generation–recombination rate is given by [13]:

$$U(x,V) = \frac{n(x,V)P(x,V) - n_i^2}{\tau_p[n(x,V) + n_1] + \tau_n[P(x,V) + P_1]} \tag{2}$$

Where n_i is the intrinsic carrier concentration and the values n_1 and P_1 are determined by the energy spacing between the top of the valence band and the generation-recombination level E_t, i.e.

$$P_1 = N_v \exp(-(E_t / kT) \tag{3}$$

$$n_1 = N_c \exp(-(E_g - E_t)/kT) \tag{4}$$

where E_g is the energy gap and N_c, N_v is the effective state densities in the conduction and valence bands, respectively and given by:

$$N_c = 2\left(\frac{m_n KT}{h^2}\right)^{3/2}, N_v = 2\left(\frac{m_p KT}{h^2}\right)^{3/2} \tag{5}$$

In this equation, m_n and m_p are the effective masses of electrons and holes, respectively.

The values $n(x, V)$ and $P(x, V)$ in Eq. (2) are the carrier concentration in the conduction and valence bands and given by [14].

$$P(x,V) = N_c \exp\left[-\frac{\Delta\mu + \varphi(x,V)}{kT}\right] \tag{6}$$

$$n(x,V) = N_v \exp\left[-\frac{E_g - \Delta\mu - \varphi(x,V) - qV}{kT}\right] \tag{7}$$

where $\Delta\mu$ is the energy spacing between the Fermi level and the top of the valence band of CdTe and $\varphi(x, V)$ is the electron energy in the space charge region is given by:

$$\varphi(x,V) = (\varphi_0 - qV)\left(1 - \frac{x}{W}\right) \tag{8}$$

According to the Eqs.(1-8), the recombination-generation current is found by integration of $U(x, V)$ throughout the entire depletion layer [16]:

$$J_{gr} = q\int_0^W U(x,V)\,dx \tag{9}$$

In addition to the recombination-generation current, there is another current which is contributing to the dark current is called the over-barrier current density J_n and can be written in the form [17]:

$$J_n = = q\frac{n_p L_n}{\tau_n}\left[\exp\left(\frac{qV}{kT}\right) - 1\right] \tag{10}$$

where n_p is the concentration of electrons in the bulk part of the p-type layer (CdTe), given by:

$$n_P = N_C \exp\left(-\frac{E_g - \Delta\mu}{kT}\right) \tag{11}$$

Thus, the dark current density in CdS/CdTe heterostructure $J_d(V)$ is the sum of the generation-recombination and over-barrier components:

$$J_d(V) = J_{gr}(V) + J_n(V) \tag{12}$$

Taking into account the effect of the series resistance (R_s) and shunt resistance (R_{SH}), the current density given by Eq.1 can be expressed as [14]:

$$J(V) = J_0\left[\left(\exp\frac{q(V + JR_S}{nkT}\right) - 1\right] + \left[\frac{V + JR_S}{R_{SH}}\right] - J_{ph} \tag{13}$$

where J_o is the saturation current density and n is the identity factor. Or simply, replacing the voltage (V) in Eqs.1-12 by $(V+JR_s)/R_{SH}$ [14].

2.2. Recombination losses

The internal quantum efficiency (η_{int}) of CdS/CdTe diode structure includes the drift (η_{drift}) and diffusion (η_{dif}) components caused by the electron-hole pair generation in the space-charge region and the neutral region of the CdTe layer, respectively. The exact solution of the continuity equation for the space-charge region and the neutral part of the CdTe layer with taking into account the drift and diffusion components and recombination at the front surface has been found in Ref. [18]. In the case of heterostructure, the solution of the continuity equation can be reduced to a simpler expression with sufficient accuracy[16]**:**

$$\eta_{drift} = \frac{1 + \frac{S}{D_p}\left(\alpha + \frac{2}{W}\frac{\varphi_0 - qv}{kT}\right)^{-1}}{1 + \frac{S}{D_p}\left(\frac{2}{W}\frac{\varphi_0 - qv}{kT}\right)^{-1}} - \exp(-\alpha W) \tag{14}$$

where S is the front surface recombination velocity; v is the applied voltage; φ_0 is the barrier height; D_p is the diffusion coefficient of hole related to their mobility μ_p by the Einstein relation $qD_p/kT=\mu_p$; W is the width of the space charge region; α is the absorption coefficient of CdTe at a given wavelength, q is the electron charge, k is the Boltzmann constant and T is room temperate. This equation takes into account losses due to recombination at the interface of CdS with CdTe, i.e. at the front surface of the CdTe layer.

The diffusion component of the quantum efficiency is also found from the continuity equation. Taking into account recombination at the back surface of the CdTe layer and it can be written as [19]:

$$\eta_{dif}=\frac{\alpha L_n}{\alpha^2 L_n^2-1}\exp(-\alpha W)\times \left\{\alpha L_n-\frac{\frac{S_b L_n}{D_n}\left[\cosh\left(\frac{d-W}{L_n}\right)-\exp(-\alpha(d-W))\right]+\sinh\left(\frac{d-W}{L_n}\right)+\alpha L_n\exp(-\alpha(d-W))}{\frac{S_b L_n}{D_n}\sinh\left(\frac{d-W}{L_n}\right)+\cosh\left(\frac{d-W}{Ln}\right)}\right\} \quad (15)$$

where $L_n=(\tau_n D_n)^{1/2}$ is the electron diffusion length; D_n is the diffusion coefficient of electron related to their mobility μ_n by the Einstein relation $qD_n/kT=\mu_n$;τ_n is the electron lifetime; S_b is the velocity of recombination at the rear surface of the CdTe layer and d is the thickness of the CdTe layer.

The internal quantum efficiency is the sum of the drift component (Eq.14) and the diffusion component (Eq.15).

Another important quantity is called the external quantum efficiency (η_{ex}) which takes into account the optical losses of the transmitted light before it reaches the absorber layer is given by:

$$\eta_{ex}=T(\lambda)\eta_{\text{int}} \quad (16)$$

More details about the transmission spectra and the optical losses will be discussed in the following section.

2.3. Optical losses

The typical structure of CdS/CdTe solar cells has a form: glass/TCO/ CdS/CdTe/ metallic back contact. Where TCO is the transparent conductive oxide layer such as SnO_2 or ITO (indium tin oxide). The solar radiation penetrates the glass substrate, a TCO layer and a CdS window layer before reaching the active CdTe absorber layer. During this path a cretin losses will be achieved caused by the reflection at interfaces; air-glass, glass-TCO, TCO-CdS and CdS-CdTe. Another losses "absorption losses" which are attributed to the absorption process in glass plate, TCO layer and CdS layer. The reflection losses and absorption losses are called the optical losses.

Calculating the transmission of spectrum ($T(\lambda)$) which reaches the absorber layer leads to estimate the optical losses. In the present case the multiple reflections effect at different interfaces will be considered. When the multi-reflections of L layers is taken into calculation, the transmission coefficient, $T(\lambda)$can be expressed in the following form [20,21]:

$$T_R=4\frac{n_1 n_2}{(n_1+n_2)^2}\prod_{j=2}^{L-1}\frac{4\frac{n_j n_{j+1}}{(n_j+n_{j+1})^2}}{\left(1-\frac{(n_j-n_{j-1})^2(n_j-n_{j+1})^2}{(n_j+n_{j-1})^2(n_j+n_{j+1})^2}\right)} \quad (17)$$

wheren_1 and n_2 are the refractive indices of the air and glass, respectively. When the absorption process has taken place in glass, ITO and CdS, Eq.(17) can be written in the form:

$$T(\lambda)=T_R(e^{-\alpha_1 d_1})(e^{-\alpha_2 d_2}) \quad (18)$$

whereα_1, α_2, d_1, and d_2 are the absorption coefficients and thicknesses of ITO and CdS layers, respectively. The absorption coefficient is calculated from:

$$\alpha(\lambda)=\frac{4\pi}{\lambda}k(\lambda) \quad (19)$$

where k is the extinction coefficient of used material.

In these calculations, the extinction coefficient of glass substrate is assumed to be equal zero, while its refractive index is calculated using Sellmeier dispersion equation [22].The extinction coefficient and refractive index data of ITO, CdS and CdTe were taken from Refs. [9], [23] and [24], respectively.

2.4. Short-circuit current density

If Φ_i is the spectral radiation power density and hv is the photon energy, the spectral density of the incident photon flux is Φ_i/hv, and then the short-circuit current density J_{SC} is given by [9, 16]:

$$J_{SC}=q\sum_i T(\lambda)\frac{\phi_i(\lambda_i)}{h\nu_i}\eta(\lambda_i)\Delta\lambda_i \quad (20)$$

where $T(\lambda)$ is the optical transmission and $\Delta\lambda_i$ is the interval between the two neighboring values λ_i. The calculations will be done for AM1.5 solar radiation using Tables ISO 9845-1:1992 (Standard ISO, 1992) [25].

The values of the parameters that were used in this work are listed in Table 1.

Table 1. The values of the parameters that are used in the present work

Symbol	Value	Ref.
d_1	100 nm	[10]
E_g	1.5 eV	[1]
Φ_0-qv	1 eV	[10]
μ_p	80 cm^2/(V S)	[15]
μ_n	1000 cm^2/(V S)	[15]
S	10^7 cm/sec	[15]
S_b	10^7 cm/sec	[15]
τ_n	10^{-9} s	[16]
d_{CdTe}	7 μm	Current work

3. Results and discussion

Fig. 1 shows the generation–recombination rate $U(x,V)$ as a function of coordinate x.$U(x, V)$ rate is calculated for different values of energy spacing between the Fermi level and the top of the valence band of CdTe ($\Delta\mu$=0.15, 0.169, 0.19 eV) at different values of forward voltage. As observed from this figure, the generation-recombination rate represents a symmetric, bill-shaped form. It can be seen that the increasing of Δμ from 0.15 eV to 0.19 eV has no significant effect on the value of $U(x, V)$.With increasing the forward bias voltage (V), the maximum peak of the curves is shifted to the front surface (x=0) of the CdTe layer. These shifts decrease with increasing the value of $\Delta\mu$. Moreover, at high voltage (V>0.8 V) and small $\Delta\mu$=0.15 eV, the front surface recombination of CdTe layer starts to take place. This means that at this value ($\Delta\mu$=0.15 eV) the barrier height for transferring the holes (majority carriers) from CdTe to CdS and for transferring the electrons (minority carriers) from CdS to CdTe represents its maximum value.It is also seen in Fig. 1 that under moderate voltages and high $\Delta\mu$, recombination at the interface can be ignored, but when qV approaches φ_o, surface recombination becomes essential [6].

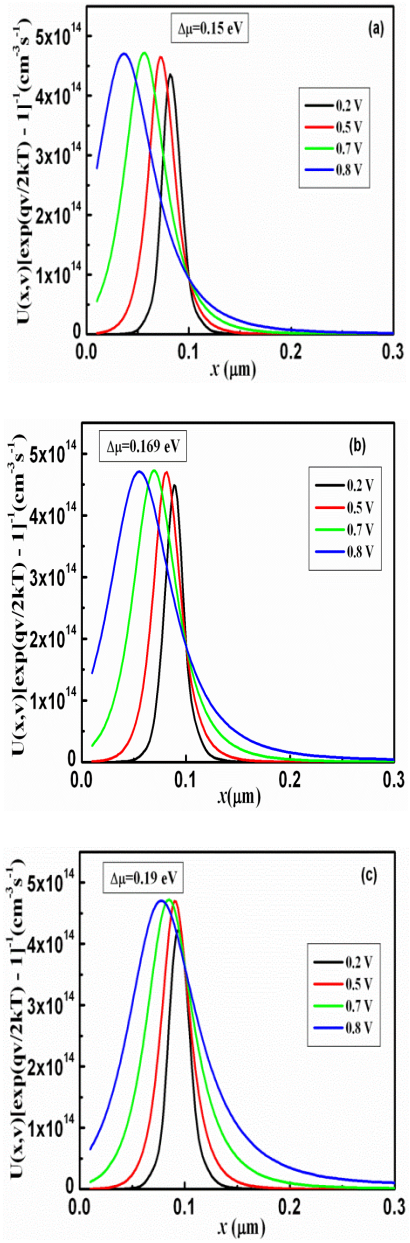

Fig. 1. The generation–recombination rate U(x,V) divided by[exp(qV/2kT)-1] as a function of coordinate x calculated for different Δμ(0.15, 0.169, 0.19 eV) at different forward voltages

Using the Eq. 12, the dark current (J_d) of CdS/CdTe heterojunction is calculated at forward bias and plotted in Fig. 2 at different temperatures. It is clear that J_d increases with increasing the temperature form room temperature to 343 K. keep in mind that these calculations are carried out in the cases of R_s=0 and R_{SH}=≡.

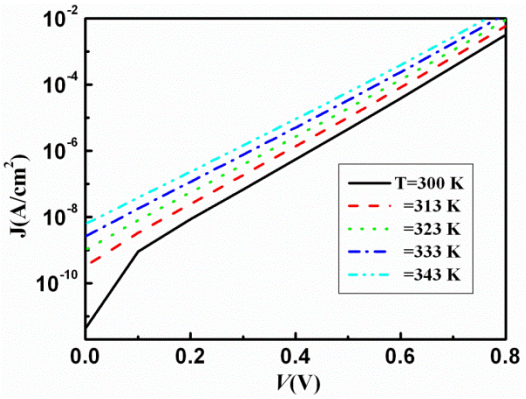

Fig. 2. Semilogarithmic plots of the forward bias of J–V characteristics at different temperature of CdS/CdTe cell

Under the above considerations and at J_{ph}=22.5 mA/cm^2, $\Delta\mu$=0.169 eV, the current density – voltage *J-V* characteristic under the illumination condition of AM1.5 solar irradiation [25] is plotted in Fig. 3 at room temperature. The *J-V* curve describes three important parameters that give complete description of the solar cell: open-circuit voltage V_o, fill factor FF(= J_mV_m/V_oJ_{SC}) and the cell efficiency η (V_mJ_m/p_{in}, p_{in}=96.3 mW/cm^2 [26]). From this figure, it is observed that the values of *Vo*, *FF* and η are 846 mV, 81% and 16%, respectively. The current–voltage characteristics of the device are largely dependent on the series R_s and shunt resistances R_{SH}. Series and shunt resistances affect the *J-V* characteristics of the solar cells, therefore determination of them is crucial. CdS/CdTe solar has a series resistance associated with it. The series resistance could be due to the resistivity of all three layers of ITO, CdS, and CdTe particularly the resistivity of CdTe layer. Shunt resistance can arise from some current paths caused by imperfections of the cell structure, like "pinholes" or as suggested in [27] from surface conduction by recombination-generation, tunneling at three-dimensional imperfections in the junction plane, etc.

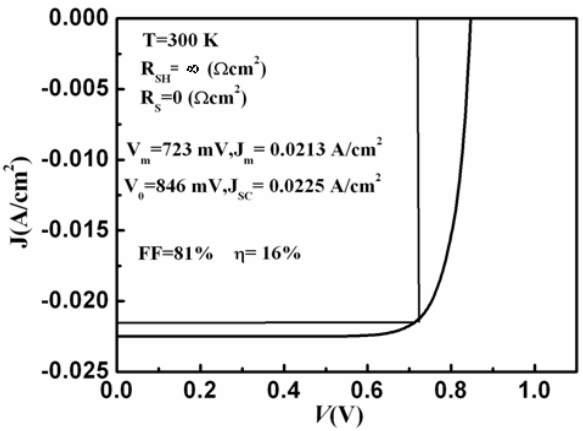

Fig. 3. J–V characteristics of CdS/CdTe heterojunction under AM1.5 solar irradiation under certain conditions

The effect of series resistance R_s on the behavior of *J–V* characteristics of CdS/CdTe heterojunction under AM1.5 solar irradiation at fixed shunt resistance R_{SH}=4000 Ω cm^2 is shown in Fig. 4. It can be seen that with increasing the series resistance the short-circuit current density decreased where the curves are shifted upward. Moreover, all curves have close values of the open-circuit voltage of about 845 mV. A similar behavior was obtained in Ref.[28]. The values of fill factor (*FF*), output power density (P_{out}) and the cell efficiency (η) are estimated from Fig. 4-a and plotted in Fig. 4-b as a function of series resistance. It is clear that all these parameters decrease with increasing the series resistance. As the series resistance increase from zero Ω cm^2 (as shown in Fig. 3) to 50 Ω cm^2, *FF* decreases from 81% to 78% with a ratio of about 4%. The cell efficiency decreases from 16% to 15.2 % with a ratio of about 5%.

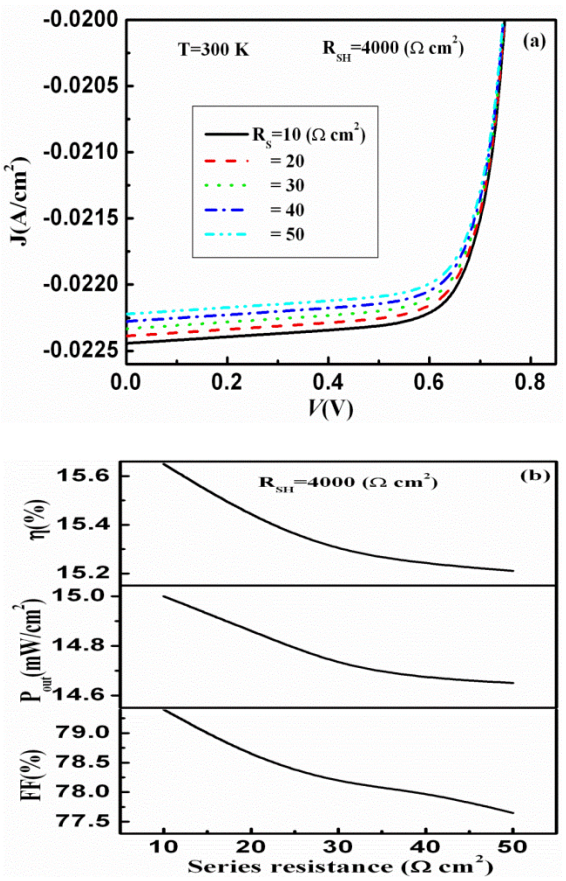

Fig. 4. The effect of series resistance R_s on the behavior of J–V characteristics of CdS/CdTe heterojunction under AM1.5 solar irradiation (a), the dependence of FF, Pout and η of CdS/CdTe cell on the series resistance (b) at fixed shunt resistance R_{SH}=4000 Ω cm^2

Fig. 5 illustrates how the *J-V* characteristic varies with decreasing the shunt resistance R_{SH} from infinity to 1000 Ω cm^2 at zero series resistance R_s. It is known that the shunt resistance should be as large as possible, so that the current that flows through it can be neglected in

comparison with that through the cell. The results presented in Fig. 5 show that all curves have close values of the short-circuit current density of about 22.5 mA/cm^2. While, the open-circuit voltage is slightly decreased from 847 mV to 844 mV, which corresponds to the variation of R_{SH} from ≡ to 1000 Ω cm^2.

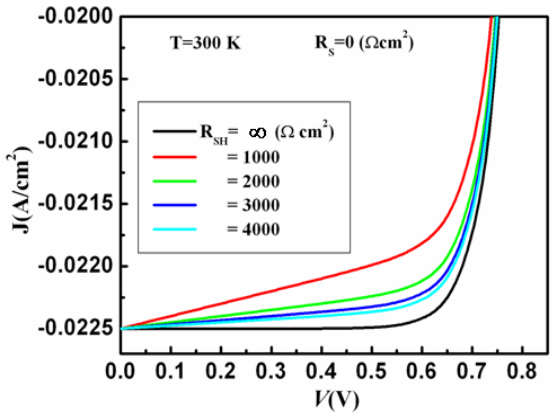

Fig. 5. The effect of shunt resistance R_{SH} on the behavior of J–V characteristics of CdS/CdTe heterojunction under AM1.5 solarirradiationat zero series resistance R_s=0 Ω cm^2

The dependence of *FF*, P_{out} and ≪ on the R_{SH} is estimated from Fig. 5 and listed in Table2. From this table it can be seen that with decreasing R_{SH} from ≡ to 1000 Ω cm^2, *FF* decreases from 80.77% to 77.5 % with a ratio of about 4%. Also the output pour density decreases with the same above ratio. While, the cell efficiency decreases by a ratio close to 5%.

Table 2. Dependence of fill factor FF, output power density P_{out} and the cell efficiency ≪ of CdS/CdTe solar cell on the shunt resistance R_{SH} at zero series resistance

R_{SH} (Ω cm^2)	*FF*(%)	P_{out}(mW/cm2)	≪(%)
1000	77.54	14.70	15.27
2000	78.20	14.85	15.43
3000	78.57	14.93	15.5
4000	78.58	14.93	15.5
≡	80.77	15.27	16

According to the above results, at the series resistance represents its maximum value of 50 Ω cm^2 and the shunt resistance represents its minimum value of 1000 Ωcm^2, the cell efficiency records a value of 15%. Comparing the results that were obtained from Fig. 3 and Fig. 5, it can be concluded that the electrical losses due to series and shunt resistance are about 6%.

Fig.6 shows the transmission spectrum $T(\lambda)$ of the glass/ITO/CdS structure calculated at 100 nm thickness of ITO and at different thicknesses of CdS. The value of transmission that is calculated using Eqs. 17-19 is achieved in the case of multiple reflection at air-glass, glass-ITO, ITO-CdS and CdS-CdTe as well as the absorption in ITO and CdS layers. The variation of $T(\lambda)$ of unity represents the losses in the transmitted light (optical losses) that will reach the absorber layer. It can be seen that the average value of *T* in the wavelength range 550-850 nm is approximately independent on the thickness of the window layer where T~0.87. This means that the optical losses is about 13% in this range. In shorter wavelength (300-550 nm), *T* is strongly dependent on the thickness of CdS. The transmission tends to decrease with increasing the thickness of CdS particularly in the high absorption region. It is clear that the decreasing of *T* with d_{CdS} is mainly due to the absorption process. The average value of *T* in the wavelength range 300-550 nm is 0.4 and 0.65 for d_{CdS}=100 and 50 nm, respectively. That indicates the transmission losses have values ranged from 60% to 35% for d_{CdS}=100 and 50 nm, respectively. The transmission losses in whole wavelength (300-850 nm) are in the range 46-29% which corresponds to the 100-50 nm thickness of CdS, respectively.

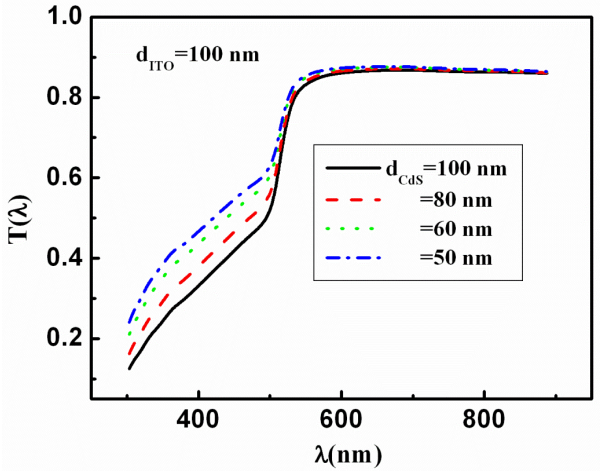

Fig. 6. Transmission spectrum T(λ) of the glass/ITO/CdS structure calculated at 100 nm thickness of ITO and different thicknesses of CdS

The effect of the optical losses on the short-circuit current density J_{SC} can be studied quantitatively through calculating J_{SC} using Eq.20 at ≪(λ)=1. The effect of the optical losses on J_{SC} is shown in Fig.7. At zero point of *x*-axis which indicates that the thickness of CdS and ITO is zero and thus this point refers only to the reflection losses. At this point, J_{SC}=28.86 mA/cm^{2}which it indicates that the reflection losses are about 8% where the maximum short-circuit current density J^0_{max} is 31.24 mA/cm^2, which is calculated at $T(\lambda)$=1 and ≪(λ)=1. When the absorption losses in both ITO and CdS are taken into account, J_{SC} decreases up to 24.8 mA/cm^2 for d_{CdS}=50 and 23.66 mA/cm^2 for d_{CdS}=100 nm at d_{ITO}=100 nm. Thus, with

decreasing the thickness of window layer from 100 nm to 50 nm, the optical losses decreased from 24% to 20%. It should keep in mind that the thickness of window layer CdS must not be less than 50 nm in order to avoid the pin-hole effect [29, 30].

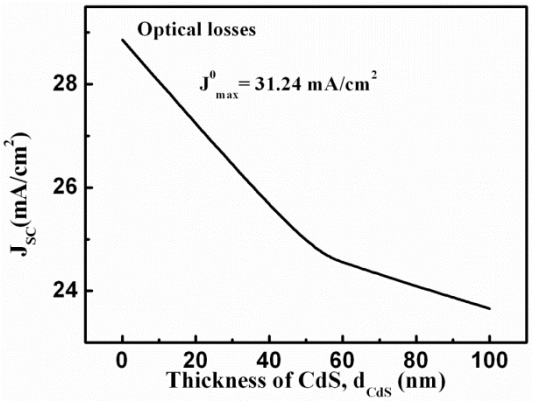

Fig. 7. Effect of the thickness of CdS(d_{CdS}) on the short-circuit current density (J_{SC}) of CdS/CdTe solar cell

Fig. 8 describes mathematically the spectral distribution of quantum efficiency (internal η_{int} and external η_{ex}) of CdS/CdTe solar cell as a function of the width of space-charge region at certain parameters of the absorber layer that are listed in Table 1. It can be observed from Fig. 8-a, the shape of internal quantum efficiency η_{int} varies with changing the width of the space-charge region *W*. When *W* increases from 0.01 μm to 10 μm, η_{int} firstly increases and then undergoes decreasing. The maximum value of η_{int} is achieved at *W*=0.5-1 μm. This behavior can be explained in terms of the width of the depletion region. The depletion layer can't collect all the photogenerated carriers at very small width. With expansion the depletion region, it becomes more efficient to collect the photogenerated carrier. However, at high width of the depletion region, the electric field becomes weaker which is favorable for the surface recombination [10]. This effect is clearly demonstrated by the curves for which *W*=5 μm and 7 μm. The external quantum efficiency η_{ex} shows also the same behavior as that of the internal quantum efficiency η_{int}, but the values of η_{ex} seem to be lesser than the value of η_{int}, particularly at low wavelength <500 nm. This behavior can be attributed to the losses of the incident photon within the front electrode layer ITO and window layer CdS as can be seen from Fig. 6 [6].

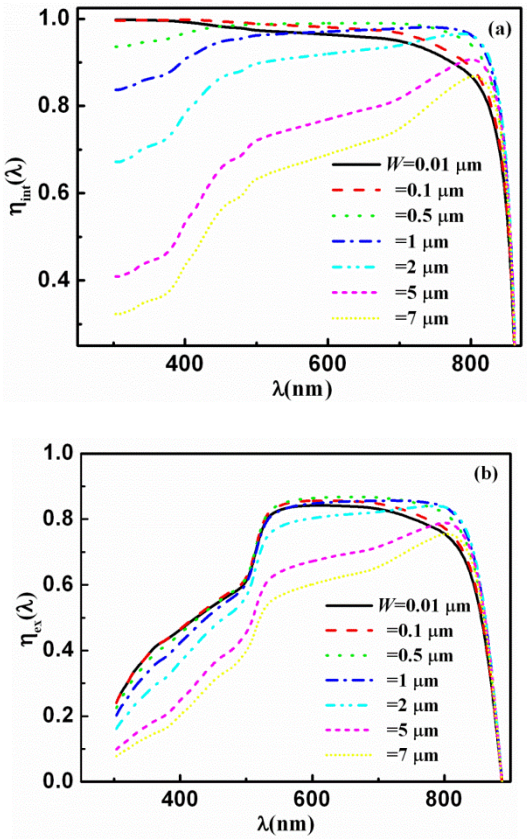

Fig. 8. Internal η_{int} (a) and the external η_{ex} (b) quantum efficiency as a function of width of space-charge region (W) for CdS/CdTe solar cell

The short-circuit current density is calculated in order to estimate the losses due to recombination in the front and back surface of CdTe layer as well as the optical losses due to reflection at interfaces of CdS/CdTe cell and absorption in both ITO and CdS layer. Fig. 9-a represents the dependence of J_{SC} on the width of space-charge region at $T(\lambda)$=1, i.e. due to recombination losses in the neutral part of CdS/CdTe heterojunction. It can be seen that J_{SC} increases with increasing *W* up to *W*=1 μm then J_{SC} starts to decrease with further increasing in *W*. These results are expected according to the results which are carried out from Fig.8. The maximum value of J_{SC} is 29.61 mA/cm^2 is achieved at *W*=0.5-1 μm. In this case, the losses arise from recombination at the surface (front and back) of CdTe are about 5%. When the depletion layer is widen (*W*>5 μm), the recombination losses increase and attain the maximum value of 27% at *W*=7 μm. Fig. 9-b shows J_{SC} as a function of *W* when optical and recombination losses are taken into accounts. It is clear that with increasing the thickness of CdS layer the values of J_{SC} decrease due to a great part of the incident photons will be absorbed in CdS layer and thus the photons reaching the absorber layer will decrease. Besides, a maximum J_{SC} of 23.6 mA/cm^2 is observed at d_{CdS}=50 nm and *W*=0.5-1 μm. At these conditions, the optical and recombination losses are about 25%. These losses can be increased with increasing the thickness of CdS layer and/or increasing the width of the space-charge region.

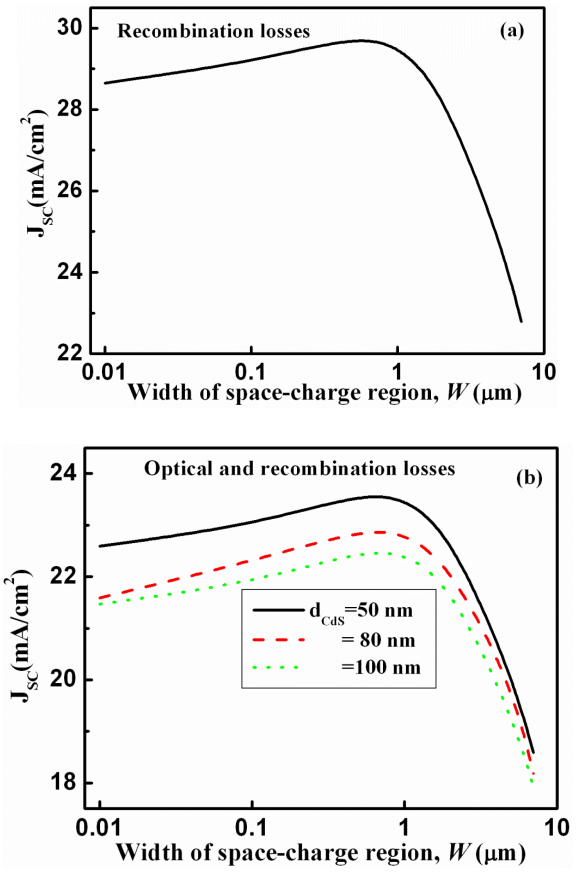

Fig. 9. Short-circuit current density J_{SC} as a function of the width of space-charge region W when the recombination losses (a) and optical and recombination losses (b) are taken into accounts

4. Conclusions

The effect of electrical, optical and recombination losses on the performance of thin-film CdS/CdTe solar cell was theoretically studied. The electrical losses arisen from series resistance and shunt resistance was analyzed. The Sah-Noyce-Shockley theory of generation-recombination in the space-charge region was employed to describe *I-V* characteristics of thin-film CdS/CdTe heterostructure. The optical losses due to multiple reflections at interfaces of CdS/CdTe cell as well as due to absorption in front contact layer and in window layer were studied. Besides, the losses due to recombination at the front and back surface of CdTe layer were considered. The obtained results showed that:

1- When the series resistance increased from zero to 50 Ω cm^2 and the shunt resistance decreased from infinity to 1000 Ω cm^2, the fill factor decreased by a ratio of 4% and the cell efficiency decreased by a ratio of 6%.
2- The optical losses were dependent on the thickness of the window layer. With decreasing the thickness of window layer from 100 nm to 50 nm, the optical losses decreased from 24% to 20%.
3- The recombination losses were affected by the width of the space-charge region. The recombination losses recorded a minimum value of 5% at width 1 μm of the space-charge region and recorded a maximum value of 27% at width7 μm.
4- The minimum optical and recombination losses were not less than 25% which can be increased with increasing the thickness of the CdS layer and/or increasing the width of the space-charge region.
5- The maximum cell efficiency of about 16% was achieved at zero series resistance and infinity shunt resistance.
6- These results are agreement with experimental studies and can lead to develop the technology of CdS-CdTe solar cells.

Acknowledgment

This project was supported by King Saud University, Deanship of Scientific Research, College of Science Research Center.

References

[1] T. Ju, L. Yang, S. Carter**,** Journal of Applied Physics **107**(10), 104311 (2010).
[2] S. Chun, S. Lee, Y. Jung, J. S. Bae, J. Kim, D. Kim, Current Applied Physics **13**(1), 211 (2013).
[3] T. Gaewdang, N. Wongcharoen, T. Wongcharoen, Energy Procedia **15**, 299 (2011).
[4] X. Wu, J. C. Keane, R. G. Dhere, C. DeHart, D. S. Albin, A. Duda, T. A. Gessert, S. Asher, D. H. Levi, P. Sheldon, Proceedings of the 17th IEEE European Photovoltaic Solar Energy Conference, Munich, Germany, 995–1000 (2001).
[5] M. A. Green, K. Emery, Y. Hishikawa, W. Warta, E. D. Dunlop, Prog. Photovolt. Res. Appl. **21**(1), 1 (2013).
[6] L. Kosyachenko, T. Toyama, Sol. Energy Mater. Sol. Cells **120**, Part B, 512 (2014).
[7] L. Zhi, F. Lianghuan, Z. Guanggen, L.Wei, Z. Jingquan, W. Lili, W. Wenwu, J. Semicond. **34**(1), 014008 (2013).
[8] L. A. Kosyachenko, E. V. Grushko, X. Mathew, Solar Energy Mater. Sol. Cells **96**, 231(2012).
[9] H. A. Mohamed, Journal of Applied Physics **113**, 093105 (2013).
[10] H. A. Mohamed, Thin Solid Films **589**, 72 (2015).
[11] W. F. Mohammed, O. Daoud, M. Al-Tikriti, Circuits and Systems **3**, 230 (2012).
[12] S. Hegedus, D. Desai, C. Thompson, Prog. Photovolt: Res. Appl. **15**(7), 587 (2007).
[13] C. Sah, R. Noyce, W. Shokley, Proc. IRE **45**(9), 1228 (1957).
[14] L. A. Kosyachenko, V. M. Sklyarchuk, O. F. Sklyarchuk, V. A. Gnatyuk, Semicond. Sci. Technol.

22(8), 911 (2007).
[15] H. A. Mohamed, J. Optoelectron. Adv. M. **16**(3-4), 333 (2014).
[16] L. A. Kosyachenko, A. I. Savchuk, E. V. Grushko, Thin Solid Films **517**(7), 2386 (2009).
[17] S. Sze, Physics of Semiconductor Devices, 2nd ed., Wiley, New York, (1981).
[18] M. Lavagna, J. P. Pique, Y. Marfaing, Solid State Electron. **20**(3), 235 (1977).
[19] S. M. Sze, K. K. Ng, Physics of Semiconductor Devices, 3rd ed., Wiley- Interscience, New Jersey 725 (2006).
[20] F. W. Mont, J. K. Kim, M. F. Schubert, H. Luo, E. F. Schubert, R. W. Siegel, Proc. SPIE 6486, 64861C (2007).
[21] F. W. Mont, J. K. Kim, M. F. Schubert, E. F. Schubert, R. W. Siegel, J. Appl. Phys. **103**(8) 083120 (2008).
[22] S. O. Kasap, Optoelectronics and Photonics: Principles and Practice, Prentice Hall, New Jersey, 2000, p.45.
[23] S. Ninomiya, Sadao, Journal of Applied Physics **78**, 1183 (1995).
[24] P. D. Paulson, X. Mathew, Solar Energy Materials and Solar Cells **82**(1-2), 279 (2004).
[25] Reference Solar Spectral Irradiance at the Ground at Different Receiving Conditions, Standard of International Organization for Standardization ISO 9845-1 (1992).
[26] T. Toshifumi, S. Adachi, H. Nakanishi, K. Ohtsuka, Japanese Journal of Applied Physics **32**(8), 3496 (1993).
[27] A. F. Fahrenbruch, R. H. Bube, Fundamentals of Solar Energy Conversion, Academic Press, New York (1983).
[28] J. L. Peña, O. Arés, V. Rejón, A. Rios-Flores, Juan M. Camacho, N. Romeo, A. Bosio**,** Thin Solid Films **520**, 680 (2011).
[29] A. Morales-Acevedo, Solar Energy **80**(6), 675 (2006).
[30] Xavier Mathew et al., Solar Energy **86**(4), 1023 (2012).

*Corresponding author: hussein_abdelhafez2000@yahoo.com